Nature Environment and Pollution Technology
An International Quarterly Scientific Journal

p-ISSN: 0972-6268
(Print copies up to 2016)
e-ISSN: 2395-3454

Vol. 21 | No. 4 | pp. 1599-1608 | 2022

Original Research Paper

https://doi.org/10.46488/NEPT.2022.v21i04.012

Open Access Journal

Preparation and Characterization of Hydrophobic Membranes and Their Seawater Desalination Performance Study by Direct Contact Membrane Distillation

Chitrakara Hegde†* and Rahul Ribeiro**
*Department of Science, Alliance University, Anekal, Bangalore, 562106, India
**Department of Mechanical Engineering, Alliance University, Anekal, Bangalore, 562106, India
†Corresponding author: Chitrakara Hegde; chitrakarahegde@gmail.com

Nat. Env. & Poll. Tech.
Website: www.neptjournal.com

Received: 16-01-2022
Revised: 02-03-2022
Accepted: 11-03-2022

Key Words:
Electrospinning
Membrane characterization
Direct contact membrane distillation
Seawater desalination
Performance study

ABSTRACT

Hydrophobic membranes prepared using Poly (tetrafluoroethylene) (PTFE) along with Poly (1,4-phenylene ether ether-sulfone) and zinc oxide nanoparticle was used in membrane distillation. To examine seawater purification, prepared polymeric membranes were evaluated, tested, and used in a lab-scale direct contact membrane distillation arrangement. These membranes which are synthesized using the electrospinning method have good mechanical and thermal stability. To understand prepared membranes' desalination performance, the physicochemical properties of the seawater were analyzed before and after membrane distillation. The salt rejection remained at 99% and the highest energy efficiency of the system observed is 67.3%.

INTRODUCTION

Most of the civilizations developed at the bank of rivers. As per chemosynthetic theory (Das et al. 2011), the evolution of life might have originated by a combination of different chemical substances with water as the platform. Though geographically 71% of water is there on earth, potable water for all is still a distant dream. For ages, mankind is trying to purify water in many ways like using heat energy, solar energy, disinfectant using copper pot, cloth, sand filtration, etc. The water purification process took a new dimension after the occurrence of the following events i. 1748, Abbe Nollet, work (Nollet 1748, Glater 1998) on water diffusion from dilute to concentrated solution ii. In 1959, Sidney Loeb and Srinivasa Sourirajan prepared the first asymmetric RO membrane from cellulose acetate for salt rejection (Loeb 1981) iii. 1980, Cadotte developed a new thin-film composite reverse osmosis membrane for single-pass seawater operation (Cadotte et al. 1980). It is noteworthy to know that many researchers are working to improve membrane desalination performance through membrane surface modification (Hegde et al. 2011).

Membrane distillation (MD) is an emerging technique for seawater desalination (Summers et al. 2012). MD is the transportation of water, consisting of a porous hydrophobic membrane, separating two aqueous solutions of a non-volatile component maintained at different temperatures (Findley 1967). In MD, due to the temperature difference, liquid-vapor interfaces are formed on both sides of the hydrophobic membrane pores. When a vapor pressure difference is created between sides of each pore, evaporation takes place at the warm interface and, after vapor is transported through the pores, condensation takes place at the cold interface. Resulted water flux occurs through the membrane in the direction from warm to cold. MD process is an easy and much more efficient process compared to other distillation techniques. MD is one of the promising candidates for the treatment of water, river water, wastewater, and seawater because this operation can be run by solar, tidal, and geothermal energy; works at room pressure; has minimal fabrication cost; marginal fouling effect (Manna 2016, Ramos et al. 2021). As reported in the literature, efficient MD can be realized with a minimum LEP (liquid entry pressure) of 2.5 bar, porosity 80-90% (Schneider et al. 1988), pore size 0.1-1 μm, contact angle < 90^o (Alkhudhiri et al. 2011, Ma & Hill 2011) and membrane thickness 2-700 μm (Eykens et al. 2016). In DCMD (Direct Contact Membrane Distillation), where the feed solution is in direct contact with the hot membrane side

surface producing evaporation at the cold-membrane surface (Khayet et al. 2005). DCMD configuration is the simplest with much stable flux rate (Hsu et al. 2002, Drioli et al. 2015) but has some points of concern like high thermal polarization, sensitivity to feed concentration, and quality of distillate depending on the hydrophobic nature of the membrane (Feng et al. 2018). DCMD configuration was extensively studied by many research groups using PTFE material with different types of feed solutions and the same configuration was found useful in seawater desalination (Table 1).

DCMD is one of the oldest modules that can perform water purification without a cooling condenser for distillation and gives the best permeate flux with optimal operational conditions (Ashoor et al. 2016).

Table 1: DCMD module in various literature.

Reference	Configuration	Material type	Feed
(Feng et al. 2018)	DCMD	PTFE	Seawater
(Ding et al. 2003)	DCMD	PTFE	Pure water
(El-Abbassi et al. 2009)	DCMD	PTFE	Wastewater
(Sakai et al. 1988)	DCMD	PTFE	Mixed waste
(Martínez-Díez et al. 1999)	DCMD	PTFE	NaCl
(Phattaranawik et al.2003)	DCMD	PTFE	Pure water
(Bhattacharya et al. 2014)	DCMD	PTFE	Simulated water
(Singh & Sirkar 2012)	DCMD	PTFE	Produced water
(Wijekoon et al. 2014)	DCMD	PTFE	Synthetic solution
(Hickenbottom & Cath 2014)	DCMD	PTFE	Hyper salty water
(Hwang et al. 2011)	DCMD	PTFE	NaCl
(Li et al. 2018)	DCMD	PTFE	NaCl
(Winter et al. 2017)	DCMD	PTFE	NaCl
(Damtie et al. 2018)	DCMD	PTFE	Wastewater
(Lyly et al. 2021)	DCMD	PTFE	Bovine serum albumin
(Zhao et al. 2017)	DCMD	-	Seawater
(Fadhil et al. 2019)	DCMD	-	Seawater
(Lee et al. 2015)	DCMD	-	Seawater
(Naidua et al. 2016)	DCMD	-	Seawater
(Duong et al. 2015)	DCMD	-	Seawater
(Shim et al. 2015)	DCMD	-	Seawater
(Rezakazemi 2018)	DCMD	-	Seawater
(Al-Obaidani et al. 2008)	DCMD	-	Seawater

MATERIALS AND METHODS

Materials and Sampling

PTFE (poly tetrafluoro ethylene) dispersion (60 wt%, 0.05 - 0.5 μm) and semitransparent beads of Poly (1,4-phenylene ether ether-sulfone) (PPEES), having a molecular weight of 35,000 and ZnO (average 50 nm size) were obtained from Sigma Aldrich. Reagent grade N-methyl pyrrolidone (NMP) was obtained from Merck-India and was used without any further purification.

For seawater desalination, raw water was collected from the Arabian Sea (Kasba Bengre, Mangalore, Karnataka, India,12°53' 22.956'N 74°48'56.844'' E). Water was taken from under one and a half meters of seawater level and large particles were removed by filtration.

Membrane Preparation

PPEES was taken in 12.5 ml NMP, the solution was stirred for 24 hours at 70 °C for completion of dissolution. With the temperature still at 70°C, different weight percentages of ZnO nanoparticles were dispersed over a period of 30 min, and then PTFE emulsion was added to the aforementioned solution while being constantly stirred for at least 3 h. This was followed by a 30-minute sonication. Solutions containing different weight % of PTFE and PPEES (90:10, 80:20, 70:30 and 60: 40) (Table 2) were prepared. For the making of composite membranes, the electrospinning unit consists of a high-voltage source, a syringe pump, and a stainless-steel collector. A 15 kV voltage is used during the electrospinning process, with a spinning distance of 15 cm and a fluid flow rate of 0.4 $mL.h^{-1}$. After more than 4 electrospinning, the membrane was separated from the collector. The electro-spun membrane was sintered in a furnace at 320°C for 20 min. A schematic diagram of the electrospinning process of membrane preparation is represented in Fig. 1.

Table 2 provides a list of the membrane's fundamental characteristics. Here, PPEES was employed to make the sheet flexible, ZnO served as a possible antifouling, and PTFE provided hydrophobicity.

In Table 1, the porosity and pore size of the membrane were determined by Capillary Flow Porometer (model CFP EX. 1500, Porous Materials Inc., USA). Contact angle (CA) with seawater measurements was made by sessile drop method using a goniometer VCA- Optima (AST products Inc., MA, USA). All prepared membranes exhibit a contact angle of more than 90° giving good hydrophobicity which is one of the essential requirements for MD. It should be noted from Table 1 that porosity and contact angle are influenced by the concentration of PTFE and ZnO.

Table 2: Basic characteristics of the prepared membrane.

Membrane code	Thickness [µm]	Membrane material			Pore size [µm]	Porosity	CA	Reference
		PTFE	PPEES	ZnO				
PZP-1	119 ± 4 µm	90%	1%	9%	0.2-1.0	75-80%	120 -123°	(Xiong et al. 2009, Greiner & Wendorff 2007, Hegde et al. 2015)
PZP-2	119 ± 4 µm	80%	10%	10%	0.4-1.2	75-80%	116-118°	
PZP-3	119 ± 4 µm	70%	10%	20%	0.5-1.3	76-77%	110-111°	
PZP-4	119 ± 4 µm	90%	9%	1%	0.6-1.4	75-79%	90-95°	

Direct Contact Membrane Distillation (DCMD)

MD investigations were carried out using self-designed and fabricated flat sheet cross-flow DCMD equipment. All membrane modules, listed in Table 1 were tested for leakage before the DCMD experiment. The prepared membrane module was assembled in the DCMD system, 1 % NaCl solution at 80°C flowed through the side at a constant flow rate between 400 - 900 mL.min^{-1}, and deionized water flowed through the tube side at room temperature. The conductivity of the distillate was monitored with a constant increasing sodium chloride flow rate. Collected distillate water does not show any increase in conductivity, confirming leak free membrane module.

The schematic experimental set-up is shown in Fig 2. The installation of DCMD consists of two water loops (feed and distillate) connected to five modules of the membrane with an inner diameter of 120 mm. Deionized water having low conductivity of less than 1µS/cm was used as the cold flow. Distillate having TDS less than 100 ppm was collected as potable water. The inlet temperature of distillate was maintained at 60-8°C and the circulating cold water temperature was maintained at 30°C. At the end of each operation, the membrane module is cleaned by flushing with a 2 L solution of 1% HCl and distilled water followed by a 2 L solution of 1% NaOH and distilled water. After repeated reproducibility tests the operating condition is summarized in Table 3. The schematic process is given in Fig. 2.

Calculations

Using the following equation, the water vapor permeation flux was calculated using the water that permeated from the DCMD over time.

$$J_v = V \times \rho / A \times t$$

where Jv is water vapor permeation flux (L.m^{-2}.h^{-1}), V is the volume of collected water (l), ρ is water density (kg.m^{-3}),

Table 3: Operational parameters and specifications for DCMD.

Operational Parameter	Specification
Warm water flow, five modules	Range [80 mL.min^{-1}]
Cold water flow, five modules	Range [60 mL.min^{-1}]
Distillate flow	10-30 L.h^{-1}
Warm water operation temperature	60-80°C
Cold water operation temperature	30°C
Max operating pressure	300 KPa

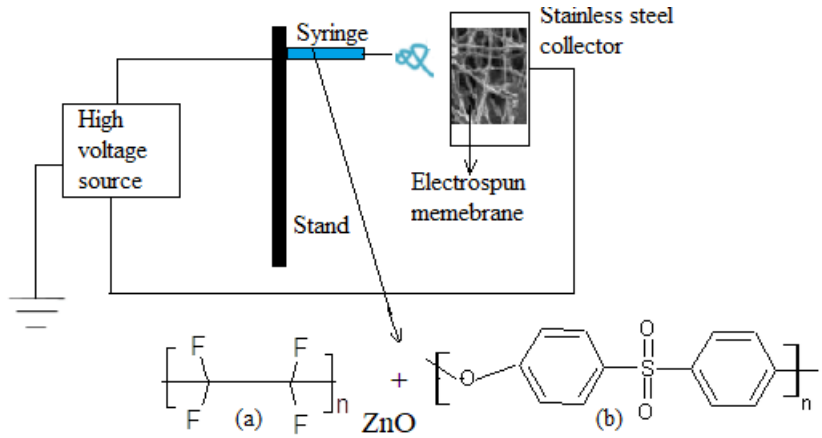

Fig. 1: Electrospinning process of membrane preparation (a = PTFE, b = PPEES) (Lalia et al. 2013).

A is the effective surface area of the membrane (m^2), and t is water collected time (h).

The salt concentrations of the feed water and permeate water into and out of the DCMD module were measured by a conductivity meter (Model DDS 307, Germany). To calculate the salt rejection, the following equation was used

$$R\ (\%) = [1-(C_p/C_f)] \times 100$$

Where 'R' is the salt rejection, 'C_P' is the concentration of permeates solution and 'C_f' is the concentration of the feed solution (Alkhudhiri et al 2011, Banat 2007).

RESULTS AND DISCUSSION

Membrane Characterization

Prepared membrane were characterized using different equipments.

Spectral Characterization

To obtain detailed information about the formation of the membranes, FT-IR spectra of the membrane are recorded using Nicolet Avatar 330 FTIR (Thermo Corporation) spec-

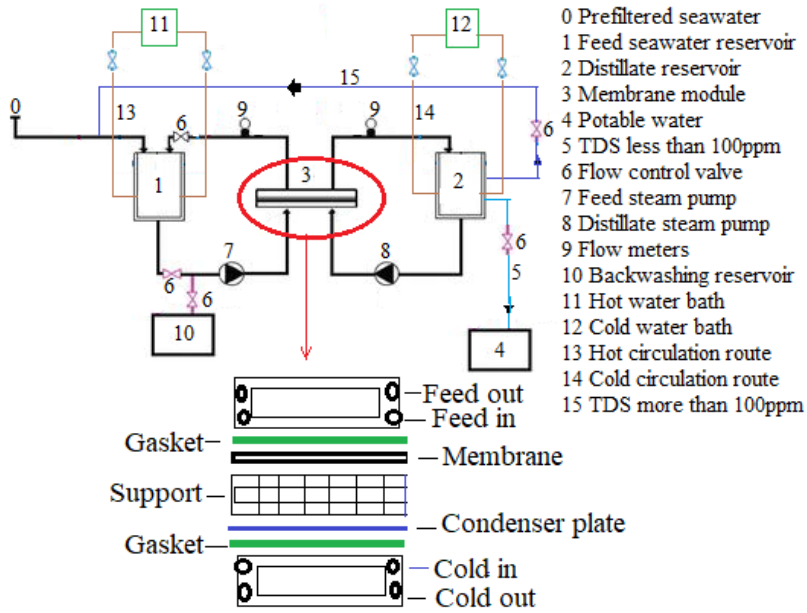

Fig. 2: Schematic DCMD process (Histov et al. 2017, Deshpande et al. 2017).

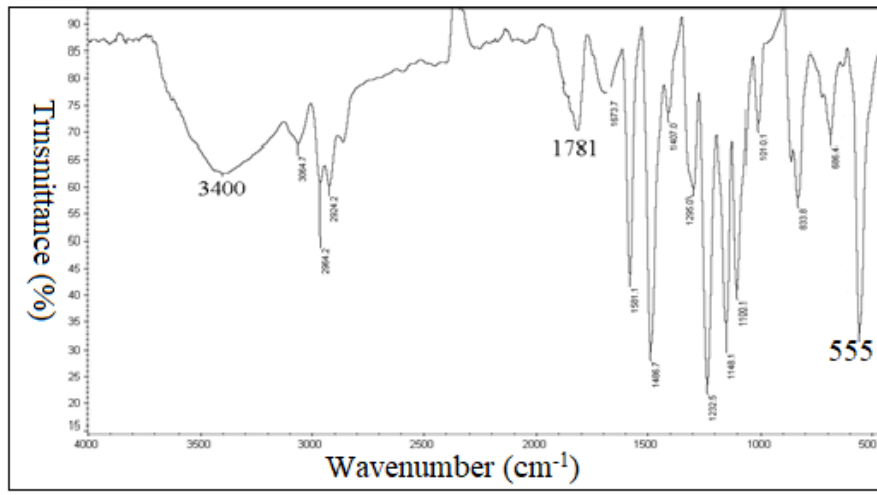

Fig. 3: IR spectrum of the PTFE-ZnO-PPEES membrane.

trometer. Fig.3 shows the IR spectrum of the PTFE -ZnO-PPEES membrane. Following stretching frequencies were observed; the carboxyl group was identified at 1781 cm^{-1}, 3600-3200 cm^{-1} for O-H stretching vibrations along with characteristic group frequencies of C - F at 630 cm^{-1}, peak at 555 cm^{-1} for ZnO (Handore et al. 2014, Li et al. 2019)

Mechanical and Thermal Study

The mechanical strength of the prepared membrane is associated with its degree of crystallinity and morphology. Membranes with poor mechanical properties may lead to early failure. The declination in mechanical strength in membranes could be due to reasons like cracks, tears, punctures, blisters stress. This paper mainly focuses on the variation of mechanical strength (young's modulus and elongation at break) and thermal properties of the membranes with respect to different times of DCMD operation (Collier et al. 2006, Ohagan 2008, Feng et al. 2016, Ranjbarzadeh-Dibazar et al. 2014). Membranes are subjected to 2 h DCMD operation (keeping cold temperature flow at 30°C and hot feed temperature at 80°C) with intervals of 20 min after each interval membranes are removed from the module and tested for young's modulus, elongation at break, and thermal property. Instron 5569 machine (Instron, USA) was used to measure young's modulus and nominal elongation at the break of the membranes. Nominal elongation break is given by:

$$\frac{\text{Elongation of the membrane under DCMD operation x 100}}{\text{Virgin membrane}}$$

The effect of desalination time on the membrane's thermal properties was investigated using Shimadzu DSC 60, Japan. For DSC analysis small piece of 5 mg of sample was placed into the crucible and the data analysis was recorded at an operating temperature of 0°C to a maximum of 200°C with a heating rate of 10°C.min^{-1}. Figs. 4 and 5, show a decrease in young modulus and elongation break with an increase in operational temperature. The decline of the nominal elongation may be due to the chain breaking of membrane materials leading to the deterioration of the membrane layer and subsequently, weakening the interaction between polymer molecules making it easy to crack. The strong C-F bond in PTFE contributes to its remarkable thermal stability, yet this study shows that the melting point of the membrane falls between 174 and 139°C. (Fig 6). This might be explained by the membranes' surface deterioration in a high-temperature area. Among all prepared membranes, the PZP-1 membrane demonstrates the best mechanical and thermal stability.

Morphology of the Membranes

The Morphology of the prepared membranes PZP-1 was studied using scanning electron microscopy (SEM). Fig.7, represents an SEM image of the membranes. The membrane's surface and cross-sectional images were recorded using Jeol JSM-84. The membrane was cryogenically fractured in liquid nitrogen and then sputtered with gold to get the membrane's image. Fig 7 (a) show evidence of linear nanofiber.

Fig 7 (b), and (c) were taken after a 6-h continuous desalination process, which exhibits stretched-apart nanofiber structure and pores deposited with other materials.

Table 4: LEP value of the prepared membranes.

Membrane code	LEP [KPa]
PZP-1	578 ± 3
PZP-2	498 ± 3
PZP-3	398 ± 3
PZP-4	297 ± 3

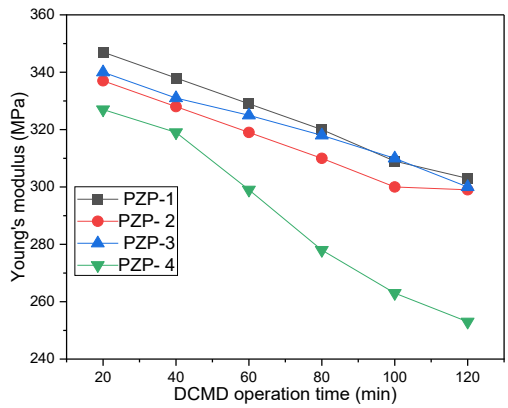

Fig. 4: Yong's modulus vs operation time.

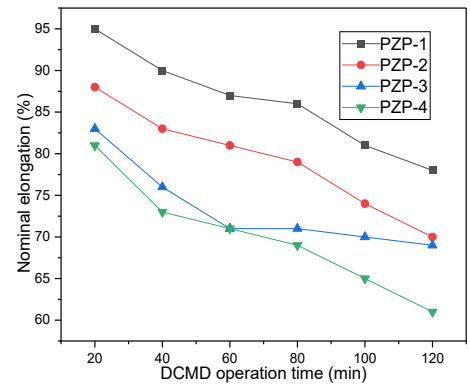

Fig. 5: Nominal elongation vs operation time.

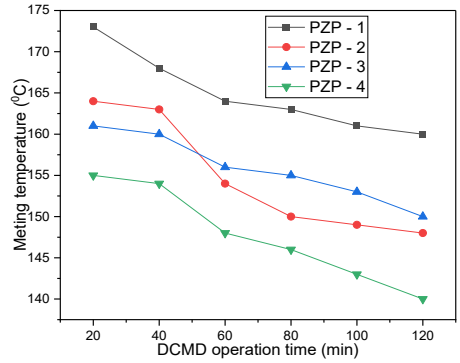

Fig. 6: Melting temperature of the membranes with different operational times.

Liquid Entry Pressure (LEP)

It is fundamental for an MD process; the applied pressure should not exceed so that the feed solution may directly enter the membrane pores. LEP depends on the pore size, membrane hydrophobicity, contact angle, surface tension, presence of organic solutes, and material used for membrane preparation (Feng et al 2018). LEP Can be calculated using the Franken equation (Franken et al. 1987).

$$\Delta P = Pf - Pp = -2B\gamma \cos\theta / r_{max}$$

Where ΔP is LEP, Pf and Pp are the hydraulic pressure on the feed and permeate side, B is a geometric pore coefficient (it is equal to1 assuming cylindrical pores), γ is liquid surface tension, θ contact angle, and r_{max} is the maximum pore size. LEP values are summarized in Table 4. All prepared membranes show sufficiently good LEP value. A significant factor in raising LEP value is the concentration of ZnO and PTFE. This may be due to PZP-1 having a high contact angle and small pore size as given in Table 2.

The DCMD Performance

After many repeated trials, the author concluded that prepared membrane PZP-1 showed good result with the self-designed, fabricated, lab scale DCMD module (Fig. 8). Table 5 exhibit the desalination performance of different membranes with the condition of cold circulation at 30°C and feed temperature 80°C. The energy efficiency (EE) of the process is obtained by the following equation

Table 5: Desalination performance of different membranes at cold temperature 30°C and hot feed temperature 80°C.

Parameter	Raw Sea-water	PZP-1		PZP-2		PZP-3		PZP-4		Instruments
		Distillate	R[%]	Distillate	R [%]	Distillate	R [%]	Distillate	R [%]	
Conductivity [μS.cm^{-1}]	55000	10-20	-	35-55	-	45-55	-	68-77	-	Model DDS 307, conductivity meter, Germany
TDS [ppm]	42600	20-30	99.9	300-400	99	425-475	99	496-515	98	HQ440 d TDS meter
Na^+ [mg.L^{-1}]	12000	0.8 -5	99.9	200-300	98-97	360-460	97-96	500-558	95	Flame photometer OFM 66 (Optima instruments)
K^+ [mg.L^{-1}]	2100	1-5	99.9	50-60	97	85-95	95	100-111	95-94	Flame photometer OFM 66 (Optima instruments)
Cl^+ [mg.L^{-1}]	18400	1-6	99.9	300-450	98-97	500-620	97-96	660-700	96	4500-Cl^- -D potentiometric methods
SO_4^{2-} [mg.L^{-1}]	1900	1-4	99.9	75-95	96-95	100-130	94-93	175-195	90-89	ASTM D4130-15
Ca^{2+} [mg.L^{-1}]	420	1-2	99.9	20-30	95-92	100-114	76-72	110-119	73-71	Flame photometer OFM 66 (Optima instruments)
Mg^{2+} [mg.L^{-1}]	1200	1-3	99.9	150-200	87-83	95-105	92-91	120-135	90-88	Flame photometer OFM 66 (Optima instruments)
EE (%)	-	67.3 ± 3		64.2 ± 3		60.1 ± 3		57.6 ± 3		

$$EE(\%) = \frac{-N\Delta H\ A}{F\ Cp\ (Ti - To)} 100$$

Where, N ($kg.m^{-2}.h^{-1}$) is the water flux, ΔH ($J.kg^{-}$) is the enthalpy of evaporation, F($kg.s^{-1}$) is the mass flow rate, A (m^2) is the effective membrane surface area, Cp ($J.kg^{-1}°C$), is the specific heat capacity of the feed solution, Ti and To are inlet and outlet bulk temperatures of the module in °C respectively (Khayet 2013, Sabbah et al. 199).

Removal efficiency (R)

Removal efficiency (R) is calculated using the following equation.

$$R(\%) = \frac{\text{Concentrate of feed} - \text{Concentrate of permeate}}{\text{Concentrate of feed}} \times 100$$

Understanding Table 5, all the membranes demonstrated good salt removal efficiency with PZP-1 producing excellent performance. Salt rejection percentage agrees with previous studies (Drioli et al. 2015, Fard et al. 2015, Francis et al. 2014). Many instruments were used to determine the different components of the raw seawater and distillate (APHA 2005). PZP-1 membrane outperformed the PZP-4 membrane in terms of desalination performance, confirming previous studies in this regard (Yong et al. 2015, Hong & He 2012, Jafarzadeh et al. 2015, Liang et al. 2012). Notably, ZnO has a superb antifouling characteristic that might be influenced by the efficient membrane distillation process. Distillate flux ($L.m^{-2}.h^{-1}$) of 6 h of desalination with PZP -1 is given in Fig. 9. Except for varying values at the beginning and conclusion, distillate flux has a nearly constant plateau at roughly 25.6 $L.m^{-2}.h$ distillate flux.

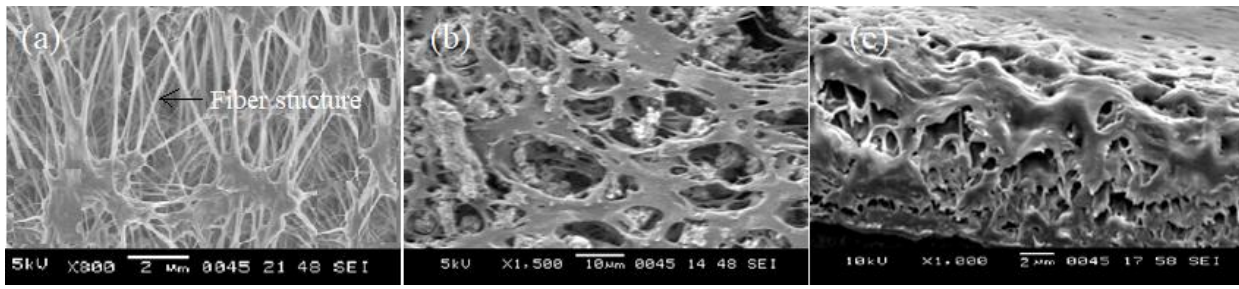

Fig. 7: SEM images of the prepared membrane (a) surface image of the membrane (b) surface image after desalination (c) cross-section image after desalination.

Fig. 8: Digital photograph of lab scale DCMD.

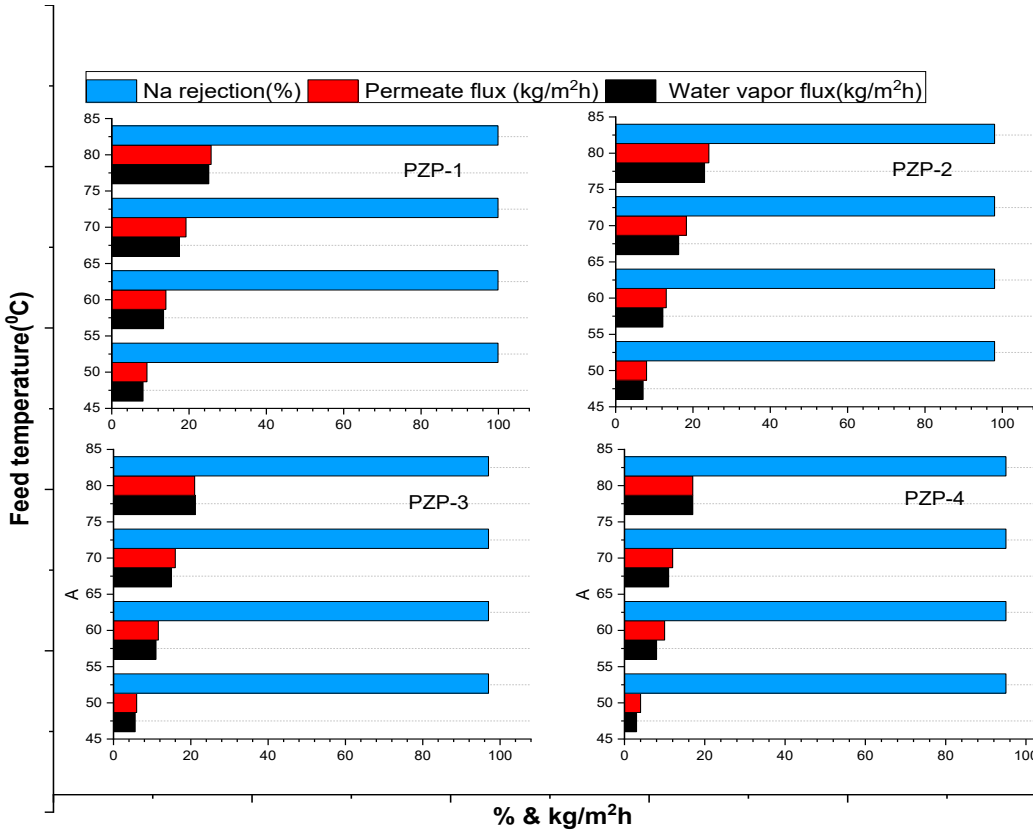

Fig. 10: Desalination performance of different membranes with feed temperature.

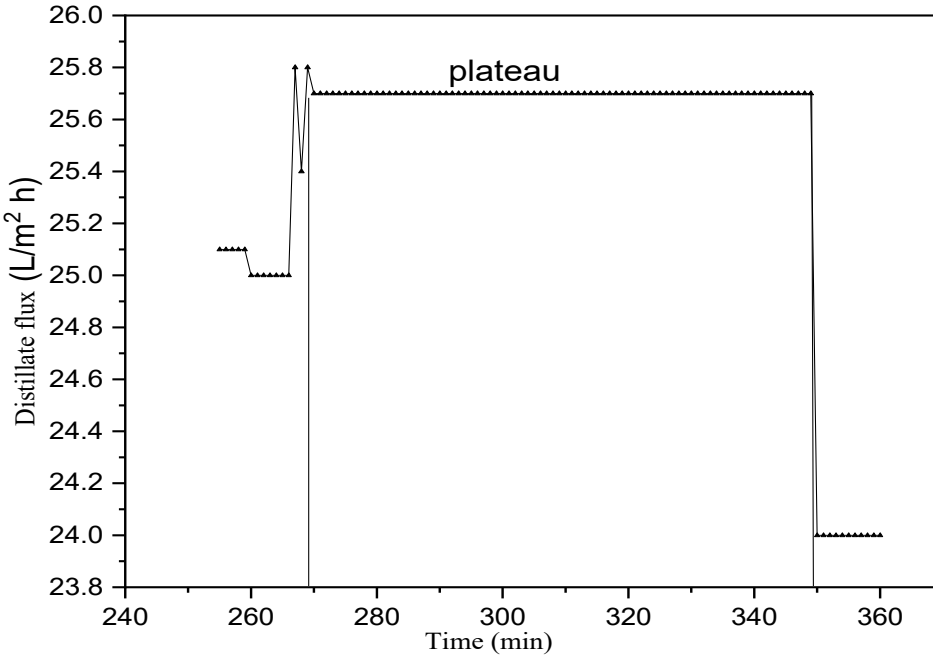

Fig. 9: 6-h Desalination process producing distillate flux with PZP-1.

From the water collected after distillation, water vapor flux (WTF) of the different prepared membranes was calculated for feed temperature at 50, 60, 70, and 80°C, maintaining a cold temperature at 30°C. Equation (1) is used to calculate WTF.

$$WTF = \frac{\text{vol.of water transferred(L)x density of water } (\frac{kg}{L})}{\text{membrane area(m2)x time (h)}} \quad \ldots 1$$

Experimentally, at cold (30°C) and feed hot temperature (80°C), PZP-1 gives the highest values for WTF, permeate flux, and sodium rejection percentage with 25.1 $kg.m^{-2}.h^{-1}$, 25.6 $kg.m^{-2}.h^{-1}$, and 99.9% respectively whereas, PZP-4 had only 17(WTF), 17.2 (permeate flux) and 95% (sodium rejection percentage) (Fig.10). Notably, all the prepared membranes depicted good salt rejection varying from 95-99.9%.

CONCLUSION

In this research work, the desalination performance of a newly prepared membrane is evaluated using lab-scale DCMD equipment. Arabian Seawater from the southern part of India was collected for this purpose. Combining prepared membrane and DCMD resulted in a highly encouraging outcome for the reduction of various components of seawater. The elimination of ions like sodium, magnesium, and potassium, in the range of 90-99%, is the best aspect of the research effort. All prepared membranes revealed a significantly respectable EE percentage. The point of contention of this work is that the data obtained in the lab scale operating conditions may require further optimization of equipment and membrane modules to reflect reality on a pilot scale. Unlike the lab scale, in the pilot scale managing high flow rate, and temperature difference between cold and hot is difficult. Irrefutably to update our module for large-scale seawater desalination further redesigning may be required.

REFERENCES

Alkhudhiri, A., Darwish,N. and Hilal, N. 2011. Membrane distillation: A comprehensive review. Desalination, 287: 2-18.

Al-Obaidani, S., Curcio, E., Macedonio, F., Profio, G.D., Al-Hinai, H. and Drioli, E. 2008. Potential of membrane distillation in seawater desalination: Thermal efficiency, sensitivity study, and cost estimation, J. Memb. Sci., 323: 85-98.

APHA, AWWA, WEF. 2005. Standard methods for the examination of water and wastewater. in: Eaton, A.D., Clesceri, L.S., Rice, E.W. and Greenberg, A.E. (eds), Centennial Edition, American Public Health Association Publication, Washington DC, pp.66-125.

Ashoor, B. Mansour, S. Giwa, A. Dufour, V. and Hasan, S.W. 2016. Principles and applications of direct contact membrane distillation (DCMD): A comprehensive review. Desalination, 398: 222-246.

Banat, F. 2007. Desalination by a "compact SMADES" autonomous solar-powered membrane distillation unit. Desalination, 217: 29 - 37.

Bhattacharya, M., Dutta, S.K., Sikder, J. and Mandal, M.K. 2014. Computational and experimental study of chromium (VI) removal in direct contact membrane distillation. J. Membr. Sci., 450: 447-456.

Cadotte, J.E., Petersen, R.J., Larson, R.E. and Erickson, E.E. 1980. A new thin-film composite seawater reverse osmosis membrane. Desalination, 32: 25-31.

Collier, A., Wang, H.J., Yuan, X.Z., Zhang, J.J. and Wilkinson, D.P. 2006. Degradation of polymer electrolyte membranes. Int. J . Hydro. Energy, 31: 1838-1854.

Damtie, M.M., Kim, B., Woo, Y.C. and Choi, J.S. 2018. Membrane distillation for industrial wastewater treatment: Studying the effects of membrane parameters on the wetting performance. Chemosphere, 206: 793-801.

Das, A., Sujith, P.P., Mourya, B.S., Biche, S.U. and Lokhabharathi, P.A. 2011. Chemosynthetic activity prevails in deep-sea sediments of the Central Indian Basin. Extremophiles, 15: 177 -189.

Deshpande, J., Nithyanandam, K. and Pitchumani, R. 2017. Analysis and design of direct contact membrane distillation. J. Memb. Sci., 523: 301-316.

Ding, Z.R., Ma, R. and Fane, A.G. 2003. A new model for mass transfer in direct contact membrane distillation. Desalination, 151(3): 217-227.

Drioli, E., Ali, A. and Macedonio, F. 2015. Membrane distillation: Recent developments and perspectives, Desalination, 356: 56 - 84.

Duong, H.C., Cooper, P., Nelemans, B., Cath, T.Y. and Nghiem, L.D. 2015. Optimizing thermal efficiency of direct contact membrane distillation by brine recycling for small-scale seawater desalination. Desalination, 374: 1-9.

El-Abbassi, A., Hafidi, A., Garcia-Payo, M. C. and Khayet, M. 2009. The concentration of olive mill wastewater by membrane distillation for polyphenols recovery, Desalination, 245: 670-674.

Eykens, L., Hitsov, I., De Sitter, K., Dotremont, C., Pinoy, L., Nopens, I. and Van der Bruggen, B.2016. Influence of membrane thickness and process conditions on direct contact membrane distillation at different salinities, J. Membr. Sci., 498: 353-364.

Fadhil, S., Alsalhy, Q.F., Makki, H.F., Figueroa, R., Marino, T., Criscuoli, A., Macedonio, F., Drioli, E., Giorno, L. and Figoli, A. 2019. Seawater desalination using PVDF-HFP membrane in DCMD process: Assessment of operating condition by response surface method, Chem. Eng. Commun., 206: 237-246.

Fard, A.K., Manawi, Y. M., Rhadfi, T., Mahmoud, K. A., Khraisheh, M. and Benyahia, F. 2015. Synoptic analysis of direct contact membrane distillation performance in Qatar: A case study, Desalination, 360: 97 -107.

Feng, S., Zhong, Z., Wang, Y., Xing, W. and Drioli, E. 2018. Progress and perspectives in PTFE membrane: Preparation, modification, and applications, J. Membr. Sci., 549: 332 - 349.

Feng, Y., Xiong, T., Xu, H., Li, C. and Hou, H. 2016. Polyamide-imide reinforced polytetrafluoroethylene nanofiber membranes with enhanced mechanical properties and thermal stabilities. Mater. Lett., 182: 59-62.

Findley, M.E. 1967. Vaporization through the porous membrane: Process design and development. Int. Eng. Chem., 6: 226-237.

Francis, L., Ghaffour, N., Alsaadi, A.S., Nunes, S.P. and Amy, G.L. 2014. Performance evaluation of the DCMD desalination process under bench scale and large-scale module operating conditions. J. Membr. Sci., 455: 103-112.

Franken, A.C.M., Nolten, J.A.M., Mulder, M.H.V., Bargeman, D. and Smolders, C.A. 1987. Wetting criteria for the applicability membrane distillation. J. Membr. Sci., 33: 315-328.

Glater, J. 1998. The early history of reverse osmosis membrane development. Desalination, 117: 297-309.

Greiner, A. and Wendorff, J. H.2007. Electrospinning: a fascinating method for the preparation of ultrathin fibers. Angew. Chem., 46: 5670-5703.

Handore, K., Bhavsar, S., Horne, A., Chhattise, P., Mohite, K., Ambekar, J., Pande, N. and Chabukswar, V. 2014. Novel green route of synthesis of ZnO nanoparticles by using natural biodegradable polymer and its

application as a catalyst for oxidation of Aldehydes. J. Macromol. Sci. Part A, 51: 941-947.

Hegde, C., Padaki, M., Isloor, M.A., Wanichapichart, P. and Liangdeng, Y. 2011. Synthesis and desalination performance of Ar^{+}-N^{+} irradiated polysulfone based new NF membrane. Desalination, 265:153 -158.

Hegde, C., Rao, S. and D'Souza, J. 2014. Synthesis of new composite polymer membrane from tapioca grains - polysulfone for desalination. Desal. Water Treat., 52: 1-8.

Hickenbottom, K.L. and Cath, T.Y. 2014. Sustainable operation of membrane distillation for enhancement of mineral recovery from hypersaline solutions, J. Membr. Sci., 454: 426-435.

Histov, I., Eykens, L., DeSchepper W., Desitter, K., Dotremont, C. and Nopens, I. 2017. Full-scale direct contact membrane distillation (DCMD) model including membrane compaction effects. J. Membr. Sci., 534: 245-256.

Hong, J.M. and He, Y. 2012. Effects of nano-sized zinc oxide on the performance of PVDF microfiltration membranes. Desalination, 302: 71-79.

Hsu, S.T., Cheng, K.T. and Chiou, J.S. 2002. Seawater desalination by direct contact membrane distillation. Desalination, 143: 279 -287.

Hwang, H.J., Gray, K.H.S., Zhang, J. and Moon, S. 2011. Direct contact membrane distillation (DCMD): Experimental study on the commercial PTFE membrane and modeling. J. Membr. Sci., 371: 90-98.

Jafarzadeh, Y., Yegani, R. and Sedaghat, M. 2015. Preparation, characterization, and fouling analysis of ZnO/polyethylene hybrid membranes for collagen separation. Chem. Eng. Res. Des., 94: 417-427.

Khayet, M. 2013. Solar desalination by membrane distillation: Dispersion in energy consumption analysis and water production costs: A review. Desalination, 308: 89 -101.

Khayet, M., Matsuura, T., Mengual, J.I. and Qtaishat, M. 2005. Design of novel direct contact membrane distillation membranes. Desalination, 192: 105-111.

Lalia, B. S., Kochkodan, V., Hashaikeh, R. and Hilal, N. 2013. A review on membrane fabrication: Structure, properties, and performance relationship. Desalination, 326: 77-95.

Lee, J., Kim, Y., Kim, W. and Francis, L. 2015. Performance modeling of direct contact membrane distillation (DCMD) seawater desalination process using a commercial composite membrane. J. Memb. Sci., 478: 85-95.

Li, K., Zhang. Y., Xu, L., Zeng, F., Hou, D. and J. Wang, J. 2018. Optimizing stretching conditions in the fabrication of PTFE hollow fiber membrane for performance improvement in membrane distillation. J. Memb. Sci., 550: 126-135.

Li, M., Chen, F., Liu, C., Qian, J., Wu, Z. and Chen, Z.2019. Electrospun fibrous PTFE supported ZnO for oil-water separation. J. Inorganic Organon. Poly. Mater., 29: 1738 - 1745.

Liang, S., Xiao, K., Mo, Y. and Huang, X. 2012. A novel ZnO nanoparticle blended polyvinylidene fluoride membrane for anti-irreversible fouling. J. Membr. Sci., 394-395: 184-192.

Loeb, S. 1981. The Loeb-Sourirajan membrane: How it came about. Syn. Membr., 53: 1-9.

Lyly, L.H.T., Ooi, B.S., Lim, W.J., Chang, Y.S., Derek, C.J.C. and Lim, J.K. 2021. Desalinating microalgal-rich water via thermo-responsive membrane distillation. J. Environ. Chem. Eng., 9: 105897.

Ma, M. and Hill, R.M. 2006. Superhydrophobic surfaces. Curr. Opin. Coll. Interface Sci., 11: 193-202.

Manna, P.P. 2016. Solar-driven flash vaporization membrane distillation for arsenic removal from groundwater: experimental investigation and analysis of performance parameters. Chem. Eng. Process. Intensif., 99: 51-57.

Martínez-Díez, L. and Vazquez-Gonzalez, M.I. 1999. Temperature and concentration polarization in membrane distillation of aqueous salt solutions. Journal of Membrane Science, 156(2): 265-273.

Naidua, G., Jeonga, S., Vigneswaran, S., Jangc, E., Choib, Y. and Hwang, T. 2016. Fouling study on vacuum-enhanced direct contact membrane distillation for seawater desalination. Desal. Water Treat., 57: 10042-10051.

Nollet, A. 1748. Lessons in Experimental Physics. Guerin Brothers, Paris, France..

OHagan, D. 2008. Understanding organofluorine chemistry. An introduction to the C-F bond. Chem. Soc. Rev., 37: 308-319.

Phattaranawik, J., Jiraratananon, R. and Fane, A.G. 2003. Effect of pore size distribution and air flux on mass transport in direct contact membrane distillatio. J. Membr. Sci., 215:75-85.

Ramos, R.L., Martins, M.F., Lebron, Y.A.R., Moreira, V.R., Reis, B.G., Grossi, L.B.and Amaral, M. C.S. 2021. The membrane distillation process for phenolic compounds removal from surface water. J. Environ. Chem. Eng., 9: 105588.

Ranjbarzadeh-Dibazar, A., Shokrollahi, P., Barzin, J. and Rahimi, A. 2014. Lubricant facilitated thermo-mechanical stretching of PTFE and morphology of the resulting membranes. J. Memb. Sci., 470: 458-469.

Rezakazemi, M. 2018. CFD simulation of seawater purification using direct contact membrane desalination (DCMD) system. Desalination, 443: 323-332.

Sabbah, R., Xu-wu, A., Chickos, J.S., Leitao, M.L.P., Roux, M.V. and Torres, L.A.1999. Reference materials for calorimetry and differential thermal analysis. Thermochim. Acta., 331: 93-204.

Sakai, K., Koyano, T., Muroi, T. and Tamura, M. 1988. Effects of temperature and concentration polarization on water vapour permeability for blood in membrane distillation. Chem. Eng. J., 38: B33-B39.

Schneider, K., Holz, W. and Wollbeck, R. 1988. Membranes and modules for transmembrane distillation. J. Membr. Sci., 39: 25-42.

Shim, W.G., He, K., Gray, S. and Moon, I.S. 2015. Solar energy assisted direct contact membrane distillation (DCMD) process for seawater desalination. Sep. Purif. Technol., 143: 94-104.

Singh, D. and Sirkar, K.K. 2012. Desalination of brine and produced water by direct contact membrane distillation at high temperatures and pressures. J. Membr. Sci., 389: 380-388.

Summers, E.K., Arafat, H.A. and Lienhard, J.H. 2012. Energy efficiency comparison of single stage membrane distillation (MD) desalination cycles in different configurations. Desalination, 290: 54 - 66.

Wijekoon, K.C., Hai, F.I., Kang, J., Price, W.E., Cath, T.Y. and Nghiem, L.D. 2014. Rejection, and fate of trace organic compounds (TrOCs) during membrane distillation. J. Membr. Sci., 453: 636 - 642.

Winter, D., Koschikowski, J., Gross, F., Maucher, D., Duver, D., Jositz, M., Mann, T. and Hagedorn, A. 2017. Comparative analysis of full-scale membrane distillation contactors - methods and modules. J. Memb. Sci., 524: 758-771.

Xiong, J. Huo, P. and Ko, F.K. 2009. Fabrication of ultrafine fibrous polytetrafluoroethylene porous membranes by electrospinning. J. Mater. Res., 24: 2755-2761.

Yong, H. E., Krishnamoorthy, K., Hyun, K. T. and Kim, S. J. 2015. Preparation of ZnO nanopaint for marine antifouling application. J. Ind. Eng. Chem., 29: 39-42.

Zhao, D., Zuo, J., Lu, K.J. and T.S. 2017. Chung, Fluorographite modified PVDF membranes for seawater desalination via direct contact membrane distillation. Desalination, 41: 119-126.